

Contact pressure dependent mechanisms of ultralow wear PTFE composites

Kylie E. Van Meter^a, Angela A. Pitenis^b, Kathryn L. Harris^c, W. Gregory Sawyer^d, Brandon A. Krick^{a,*}

^a Department of Mechanical Engineering, Florida A&M University - Florida State University College of Engineering, Tallahassee, FL, 32310, USA

^b Materials Department, University of California, Santa Barbara, CA, 93106, USA

^c RISE Research Institutes of Sweden, Stockholm, Sweden

^d Department of Mechanical and Aerospace Engineering, University of Florida, Gainesville, FL, 32611, USA

ARTICLE INFO

Handling Editor: Dr. M Dienwiebel

Keywords:

Polytetrafluoroethylene
PTFE
Alumina
Ultralow wear
Contact pressure
Tribochemistry

ABSTRACT

One of the most dramatic reductions in the wear of PTFE has been achieved by compositing PTFE with as little as 1–5 wt% of alumina particles; this has been reported to produce wear rates $K \sim 10^{-7} \text{ mm}^3/\text{Nm}$. The mechanisms associated with this reduction in wear are multifaceted, including 1) preventing crack propagation and delamination of the PTFE wear surface, 2) promoting tribochemistry and more recently 3) tribologically-induced breaking of the filler into nanoscale fragments to stabilize and reinforce tribofilms. However, in an effort to keep experiments comparable, many of the studies throughout the literature have focused on a narrow contact pressure range. In these experiments, we explored the effects of contact pressure on the tribological behavior of different PTFE and alumina composites, one of which is reported to achieve ultra-low wear ($\sim 10^{-7} \text{ mm}^3/\text{Nm}$) and another that is reported to only have mild reductions in wear ($\sim 1 \times 10^{-5} \text{ mm}^3/\text{Nm}$) compared to unfilled PTFE ($\sim 4 \times 10^{-4} \text{ mm}^3/\text{Nm}$). We found that with decreased contact pressures, the PTFE-alumina composite that was previously reported as high wear could achieve ultralow wear rates. The PTFE-alumina composite previously reported to achieve ultralow wear achieved ultralow wear at a range of low to high contact pressures, with a higher pressure limit corresponding to increases in wear. The friction behavior of PTFE-alumina composites was found to be highly dependent on contact pressure, with increasing pressures resulting in decreasing friction coefficients (~ 0.5 – 0.17 over a 0.62 – 8.5 MPa range). This effect became more pronounced when the contact pressure was incrementally varied during testing resulting in up to a 70% decrease or increase in friction coefficient due to increasing or decreasing the pressure, respectively. IR spectra of the polymer wear surface showed that tribofilms rich in carboxylates and metal oxides form at the full range of contact pressures tested, even at the extremes. This formation of tribofilms at the sliding interface not only contributes to the ultralow wear of these materials, but plays a role in the friction behavior observed. From this, we gained new insight into the role, functionality and limitations of the alumina fillers.

1. Introduction

The friction and wear of polytetrafluoroethylene (PTFE) have been central topics of the materials tribology community since PTFE's accidental creation and discovery of its remarkably low coefficient of friction [1–4]. However, PTFE's high wear rate ($K \sim 10^{-4} \text{ mm}^3/\text{Nm}$) under engineering sliding conditions [5–7] limits its use in many tribological applications. Filler materials of many materials, sizes, and shapes have been shown to reduce the wear of polytetrafluoroethylene (PTFE) by up to 10,000x [5–24]. One of the most dramatic reductions in the wear of

PTFE has been achieved by compositing PTFE with as little as 1–5 wt% of certain alumina particles; this has been reported to produce wear rates of 1×10^{-7} – $5 \times 10^{-8} \text{ mm}^3/\text{Nm}$ [17,19–23,25–27]. Fillers like alumina appear to contribute to wear reduction through the prevention of subsurface cracking and delamination, reducing debris filler size, facilitating tribochemistry, and reinforcing the polymer wear surfaces and transfer films formed during sliding.

Tribofilms of ultralow wear PTFE composites ($K \sim 10^{-7} \text{ mm}^3/\text{Nm}$) usually have chemical species present that are not found in the bulk polymer composite. Shear-induced polymer chain scission of PTFE C–C

* Corresponding author. Department of Mechanical and Aerospace Engineering, FAMU-FSU College of Engineering, Tallahassee, FL, 32310, USA.

E-mail addresses: kevanmeter@fsu.edu (K.E. Van Meter), apitenis@ucsb.edu (A.A. Pitenis), kathryn.harris@ri.se (K.L. Harris), bkrick@eng.famu.fsu.edu (B.A. Krick).

bonds as well as reactions with the environment and the sliding countersurface can generate carboxylic acid end groups, which can be found using IR spectroscopy [28–30]. In addition to the chemical changes at the sliding interface, the alumina filler has been found to accumulate at the sliding interface, leading to higher hardness and elastic moduli of the polymer wear surface in comparison to the bulk polymer [30]. These previous studies have shown that not only are the films chemically altered during sliding, but their mechanical properties change as well, leading to improved wear resistance of the composite.

The structure and mechanical properties of the alumina filler itself have been found to be a large contributor to the low-wear behavior of PTFE-alumina composites [17,30,31]. If the alumina is too dense, the particles will only serve to reinforce the bulk composite but can abrade

nanostructured 1 μm α alumina composite. The second filler was an Alfa Aesar alpha-phase alumina powder (Stock #42573) with a supplier-specified average particle size range of 0.35–0.49 μm , referred to as 0.5 μm α alumina [19,21] and size characterized in Ref. [32], but also used in Refs. [17,19,21,22]. The third filler was Nanostructured and Amorphous Materials, Inc. (Stock #1015WW) 99.5%, with a median size of ~4 μm as measured by static light scattering, referred to as nanostructured 4 μm alumina [26,32,34–36]. This filler has a porous/agglomerated architecture with nanoscale features. These powders were selected because the nanostructured 1 μm alumina and the nanostructured 4 μm alumina produced ultra-low wear PTFE composites, while the 0.5 μm alumina provided only moderate reductions in the wear rate of PTFE [19,21].

Alumina Type		Vendor Reported [32]	Static Light Scattering [32]	Tribological properties at ~6.25 MPa contact pressure [32]		Literature References
Shorthand Notation	Source	Particle Size (nm)	Median Particle Size (nm)	Wear Rate $\times 10^{-6}$ (mm^3/Nm)	Friction Coefficient	
nanostructured 1 μm	Alfa Aesar #44652	"60–80"	781	0.089	0.22	Referred to as 80 nm particle in Refs. [17, 19,21,22,24]. Size measured in [32]
dense 0.5 μm	Alfa Aesar #44573	"350–490"	267	26.00	0.18	Referred to as 0.5 μm particle in Refs. [19,21]. Size measured in [32]
nanostructured 4 μm	Nanostructured and Amorphous Materials #1015WW	"27–43"	3950	0.057	0.20	Referred to as 27–43 nm in Refs. [34–36]. Size measured in [32]

the countersurface and tribofilms. These types of alumina particles typically only reduce the wear of PTFE by 10–100x. However, if the particles are friable and can be broken down during sliding, nanoscale alumina fragments will not abrade the tribofilms and can accumulate at the interface, and the micron scale aggregates can reinforce the bulk polymer [17,32]. This breakdown of alumina particles to nanoscale sized fragments is crucial for creating ultralow wear composites, and these friable alumina particles can reduce the wear of PTFE by 10,000x. While the development of transfer films has been found to be very dependent on particle size and environmental factors, little is understood about the contribution of contact pressure to the ultralow wear behavior of these composites and the tribofilms needed to maintain it.

This study is designed to investigate the effects of externally applied contact pressure on the sliding wear of PTFE and PTFE-alumina composites. Perhaps the best example of the effects of contact pressure on the wear of PTFE was Uchiyama and Tanaka [33], where the authors evaluated the dependence of the wear of unfilled PTFE on pressure and sliding velocity. This paper showed that “linear wear rate,” α (in units [cm/cm^3]) increased with increasing contact pressure and sliding velocity, and was essentially governed by a master curve linked to temperature. It is hypothesized that the wear of PTFE-alumina composites could have a similar, if not increased, dependence on load. In these experiments, we explored the effects of contact pressure on wear rate for three different PTFE and alumina composites, two of which are reported to achieve ultralow wear ($\sim 5 \times 10^{-8}$ – $1 \times 10^{-7} \text{ mm}^3/\text{Nm}$) and another that is reported to only have mild reductions in wear ($\sim 1 \times 10^{-5} \text{ mm}^3/\text{Nm}$) [19,21].

2. Materials and sample preparation

Unfilled PTFE and PTFE-alumina composites were made using DuPont Teflon® PTFE 7C resin. Three alumina fillers were used in this study. The first filler used was an Alfa Aesar alpha-phase alumina powder (Stock #44652) with a supplier-specified average particle size of 60–80 nm, later shown to be much larger, with a median particle size of ~781 nm [32]. This particle source has three prominent peaks when looking at the size distribution (centered at 250 nm, 1 μm and 4 μm) [32], and for simplicity will be called “nanostructured 1 μm ” alumina and composites with this filler will be referred to as a PTFE with

PTFE powder was combined with 5 wt% alumina powder and initially mixed by hand. The mixture was then dispersed in isopropanol (~5:1 ratio of isopropanol to powder by mass) using a sonicating horn (Branson Digital Sonicator 450 with microtip attachment at 40% amplitude). Sonication was performed for three 5 min intervals, with 1 min rests in between to allow the sample to cool to room temperature. The dispersion was dried in a fume hood for 3–5 days to allow the isopropanol to fully evaporate.

Approximately 10g of dried powder was placed in a cylindrical mold (12.7 mm in diameter) and compression molded to 10 MPa of pressure using a hydraulic press. The molded cylinders were wrapped in aluminum foil and free sintered in an oven using the following temperature profile: 2 °C/min ramp from room temperature to 380 °C, 3 h hold at 380 °C, 2 °C/min ramp from 380 °C to room temperature. The sintered cylinders were machined into 6.3 \times 6.3 \times 12.7 mm pins to be used for testing. Prior to testing, the pins were sonicated in methanol for 30 min and allowed to fully dry in a fume hood.

The PTFE and PTFE-alumina composites were slid against 304L stainless steel rectangular flat counter samples (38 mm \times 25 mm \times 3.7 mm) with an average roughness of approximately 150 nm, which was measured using a scanning white light interferometer. These are a standard counter sample used for many previous studies of these and other PTFE composites [7,17,20,22–24,26,37,38]. Prior to testing, each counter sample was washed with Alconx soap and then rinsed with methanol. The counter samples were placed in a fume hood to fully dry.

3. Experimental methods

A linearly-reciprocating tribometer was used for all wear experiments [7,39,40]. Normal forces and friction forces were actively measured using a load cell, and servo-on-load was utilized to maintain constant normal loads throughout the course of testing. The polymer sample was pressed against the counter sample and normal loads of 12.5, 25, 50, 80, 125, 250, 500 and 1000 N were applied to the ~40 mm^2 interface, resulting in nominal contact pressures of 0.31, 0.63, 1.25, 1.93, 3.13, 6.25, 12.5 and 25.0 MPa respectively. It is important to note that several of the pressures are greater than or on the order of the

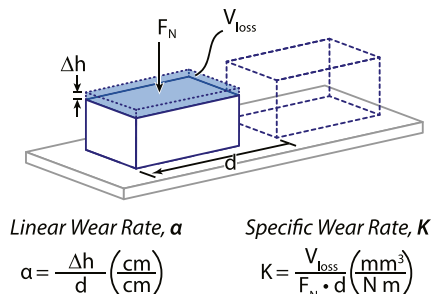
yield strength of the polymer. In some cases, the polymer deformed to have an increased apparent contact area and accommodate the load; the actual nominal contact pressures were calculated by dividing the applied normal load by the deformed end of the polymer sample at its sliding surface, which was measured with calipers after testing.

The counter sample was driven directly by a motorized linear ball-screw stage, which reciprocated with a stroke of 25.4 mm at a rate of 50.8 mm/s. With the exception of applied contact pressure, tribological sliding conditions were chosen to be the same as previous studies [7,17, 23,41–43] to match engineering conditions and to simplify comparisons between studies. Friction coefficients have an uncertainty of less than 0.005 [40], but typically have higher variations as a function of sliding cycle. Friction and wear testing was performed under unlubricated sliding conditions in lab air at room temperature (18–24 °C) and a relative humidity between 30 and 50%, which was monitored and measured during testing.

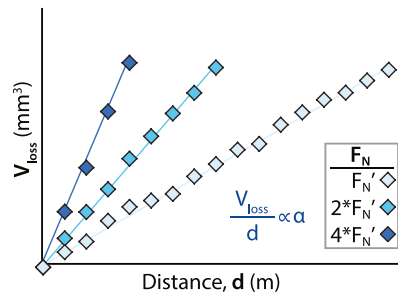
Prior to testing, the densities of the composites, ρ [g/mm³], were calculated for each polymer sample by dividing the measured initial mass of the polymer pin [g] by the dimensions of the polymer pin [mm³], measured using calipers (Mitutoyo AOS, 0.01 mm resolution). The wear of the polymer sample was monitored through intermittent mass measurements of the polymer using a Mettler Toledo scale with a resolution of 10 µg. After each incremental set of sliding cycles, the polymer sample was removed from the tribometer and weighed, similar to testing methods described in Refs. [26,28,29,37]. Mass measurements were used to quantify wear instead of using dimensional changes (i.e., height loss) in order to exclude effects of sample thermal expansion and creep. The wear volume of the polymer, V_{loss} , was calculated using the change in mass, m_{loss} , and the density of the composite, ρ . Wear rates are calculated by dividing the volume lost during sliding, V_{loss} [mm³], by the normal force, F_N [N], times the sliding distance, d [m], resulting in a specific wear rate, K [mm³/Nm] as shown in (Eq. (1) and Fig. 1) [39,40, 42,44]. Steady-state wear rates and associated uncertainties were calculated using a Monte Carlo technique [42]; uncertainties in wear rates are an order of magnitude lower than the wear rates themselves and are often smaller than the data points shown on the plots.

$$K \left[\frac{\text{mm}^3}{\text{Nm}} \right] = \frac{V_{loss} [\text{mm}^3]}{F_N [\text{N}] d [\text{m}]} = \frac{m_{loss} [\text{g}]}{\rho \left[\frac{\text{g}}{\text{mm}^3} \right] F_N [\text{N}] d [\text{m}]} \quad (1)$$

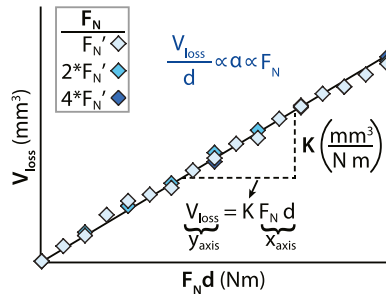
a) Linear and Specific Wear Rate



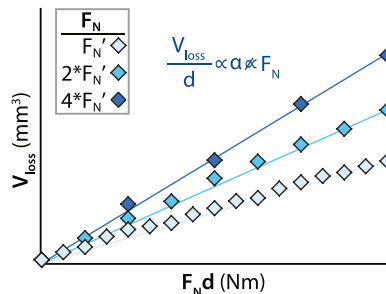
b) Idealized Volume Loss vs. Distance



c) Load-Independent Specific Wear Rate, K



d) Load-Dependent Specific Wear Rate, K



Wear rate calculations and visualizations are summarized in Fig. 1a. In Fig. 1b, a plot of volume loss vs. sliding distance is shown for idealized wear data for experiments using three different arbitrary applied normal loads (F_N : F_N , $2*F_N$ and $4*F_N$). The slope of each of these lines is proportional to the linear wear rate, α [cm/cm], as reported by Uchiyama and Tanaka. Perhaps a better way to plot this information is to plot volume loss [mm³] vs. the product of normal force and sliding distance (in Nm) as shown in Fig. 1c and d. In these plots, the slope of the data is the wear rate, K [mm³/Nm] as described in Eq. (1). Fig. 1c shows the idealized wear for a material with a constant wear rate (or coefficient of wear as described by Archard and Hirst) that does not depend on contact pressure. Fig. 1d shows the case when the material no longer has a constant coefficient of wear, but instead has a wear rate that is dependent on contact pressure. These figures are used to illustrate that it may be more appropriate to match sliding distance x normal load (or sliding distance x contact pressure) when evaluating wear of materials with varying contact pressures; this is done in an attempt to wear comparable volumes of material during sliding and allow comparable opportunity to develop transfer films and tribofilms.

A PerkinElmer Spectrum 100 Fourier Transform Infrared (FT-IR) Spectrometer with an Attenuated Total Reflectance (ATR) accessory was used to measure and identify the chemical changes to the polymer composite that occurred as a result of sliding. Both the sliding surface (tested surface) and the bulk polymer (untested surface) were measured. Spectra was collected at a spectral resolution of 4 cm⁻¹ with 32 scans per measurement. Prior to the measurement, the ATR crystal was cleaned with isopropyl alcohol, immediately followed by a background scan. The entire polymer sample wear surface was placed in contact with the diamond crystal and a normal force was applied with a torque limited probe, resulting in a spectra representative of the entire surface. The same method was used to measure an untested surface of the sample to measure the bulk, unslid composite. The PerkinElmer Spectrum software's baseline subtraction feature was used to process the raw spectra data.

Fig. 1. a) Wear rate calculation schematic for linear wear rate, α , and specific wear rate, K . b) Idealized volume loss vs. sliding distance data for wear experiments of a material with three different applied normal loads (F_N : F_N , $2*F_N$ and $4*F_N$) or contact pressures; the slope of this data is proportional to α . c) Example of idealized volume loss vs. sliding distance times normal force data for wear experiments of a material with a load-independent wear rate (K); the slope of this data is the wear rate, K . d) Example of idealized volume loss vs. sliding distance times normal force data for wear experiments of a material with a load-dependent wear rate (K).

4. Results and discussion

4.1. Summary of steady-state wear rates

Steady-state wear rates for unfilled PTFE, PTFE filled with 5 wt% nanostructured 1 μm alumina, PTFE filled with 5 wt% 0.5 μm alumina, and PTFE filled with 5 wt% nanostructured 4 μm alumina are plotted against contact pressure in Fig. 2. These wear rates and wear rate uncertainties were calculated based on intermittent mass measurements and a Monte Carlo statistical analysis. The contact pressures are based on the measured normal load and measured contact area dimensions, and error bars reflect contact pressure uncertainty calculated using propagation of uncertainty. Unfilled PTFE appears to have some minor load dependence, with marginal increases from 1×10^{-4} to 7×10^{-4} mm^3/Nm with increasing contact pressure. In contrast, the PTFE filled with 0.5 μm alumina and 80 nm alumina have load dependence when certain contact pressure thresholds are passed. For the 0.5 μm alumina, this threshold appears between 1.25 and 6.25 MPa. For the nanostructured 1 μm alumina, when contact pressures exceed 6.25 MPa, the wear rates of the samples increase by several orders of magnitude. However, for PTFE filled with nanostructured 4 μm alumina, this transition to high wear is not evident, with only a minor increase to 2.3×10^{-7} mm^3/Nm at ~ 8.5 MPa from 9.8×10^{-8} mm^3/Nm at 6.25 MPa. Results and discussion of each composite are broken out below in more detail.

4.2. Wear of unfilled PTFE

Unfilled PTFE was subjected to various nominal contact pressures during wear testing. Volume loss due to wear is shown as a function of sliding distance times normal force (F_{ND}) on a logarithmic scale (Fig. 3a) and as a function of F_{ND} on a linear scale (Fig. 3b). The volume loss due to wear appears to be linear when plotted against the product of normal force and sliding distance for each test. PTFE wears at a constant wear rate, $K \sim 6 \times 10^{-4}$ mm^3/Nm , for nominal applied contact pressures of 25, 12.5, 6.25 and 3.13 MPa. This is evident by the overlapping of the volume vs. sliding distance \times normal force plots for these pressures in Fig. 2b, similar to the idealized data in Fig. 1c. At contact pressures

below 3.13 MPa, there is a monotonic reduction in wear rate with reduction in applied contact pressure.

4.3. Wear of PTFE filled with nanostructured 1 μm alumina and nanostructured 4 μm alumina

Volume loss due to wear at various contact pressures is plotted vs. sliding distance \times normal force for PTFE and 5 wt% nanostructured 1 μm alumina composites in Fig. 4 a-c (left side of Fig. 4) and for PTFE and 5 wt% nanostructured 4 μm alumina composites in Fig. 4 d-f (right side of Fig. 4). When plotted on a linear scale large enough to visualize the entire dataset (Fig. 4b), experiments with nominal applied contact pressures of 12.5 and 25 MPa follow close to the y-axis, while experiments at pressures of 6.25 MPa and lower follow along the x-axis. This shows that the wear of PTFE with nanostructured 1 μm alumina was disproportionately greater at pressures of 12.5 and 25 MPa than at pressures of 6.25 MPa and lower. Fig. 4a is the volume lost due to wear vs. sliding distance \times normal force in log-log scale to better visualize the experiments, which span several orders of magnitude in wear volume.

Fig. 4c and f are linear and cropped to show volume loss details for 0.31, 1.25, 3.13 and 6.25 MPa nominal contact pressures. Recall that for a material that truly follows Archard's wear law, with a wear rate, k , that is independent of contact pressure, the volume loss vs. normal force times sliding distance data should be linear with the same slope for all experiments as in Fig. 1c. PTFE filled with nanostructured 1 μm alumina is different from this idealized case in two major ways: 1) The wear is not linear, with the exception of the experiment at a nominal contact pressure of 25 MPa. 2) The wear data does not share a common slope, even at steady state.

The PTFE filled with 1 μm nanostructured alumina was initially presented by Burris and Sawyer with remarkably low wear [17]. Since then, significant efforts have gone into understanding why that filler created such a wear resistant composite [17,23,24,28–30,35,45–48]; a major motivating factor was that the supplier stopped making the one alumina powder that produced significantly lower wear rates. A multi-lab effort (including various combined and independent efforts lead by the labs of Greg Sawyer, David Burris, and Brandon Krick) resulted in the nanostructured 4 μm alumina discussed here. Interestingly, the composite with 4 μm alumina has comparable wear rates to the 1 μm alumina across most contact pressures. There are two major differences, both of which are likely due to the alumina's particle size. The first is that the 1 μm alumina composites generally have less run-in wear volume. We posit that a large part of run-in for this system is the breaking down and accumulation of alumina fillers in the tribofilms (transfer film on the steel and tribofilm on the wear surface of the polymer) [32]. As the alumina particles are added to PTFE on a per-mass basis, there are a significantly greater number of particles in the 5 wt% 1 μm alumina composite compared with the 4 μm alumina. As such, it is expected that the alumina left behind and accumulated as the PTFE matrix wears during run-in forms a more uniform layer of alumina (as shown in the microtomography work in Ref. [32]) with less overall removal of composite.

The other major difference is that the 4 μm alumina wear rate does not begin to increase until contact pressures are much greater than those of the 1 μm alumina composites. This is attributed to better mechanical reinforcement of the larger, more porous 4 μm alumina filler particles. Again, because they are added to the PTFE composite on a per-mass basis, these large nanostructured 4 μm alumina particles fill a larger volume than the 1 μm alumina particles and can reinforce the bulk PTFE matrix.

While attempts were made to perform experiments at selected nominal contact pressures, it was unavoidable that the actual applied contact pressures vary and differ from the desired nominal pressures, especially for pressures near or greater than the material yield strength. To accommodate this variation, the area of the worn surface of the polymer samples were measured before and after testing, allowing for

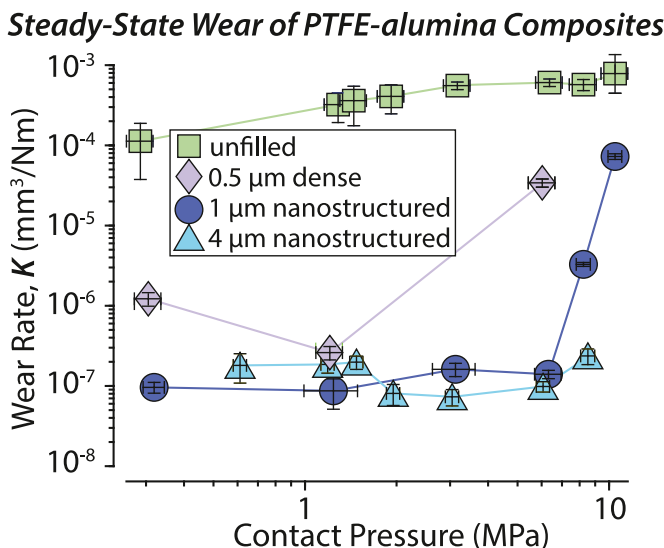


Fig. 2. Wear rate as a function of contact pressure for unfilled PTFE, PTFE filled with 5 wt% nanostructured 1 μm alumina, PTFE filled with 5 wt% nanostructured 4 μm alumina, and PTFE filled with 5 wt% 0.5 μm alumina. Contact pressure is based on measured normal load and measured contact area dimensions, and error bars reflect uncertainty in area and load. Error bars for the reported wear rates are calculated using Monte Carlo technique.

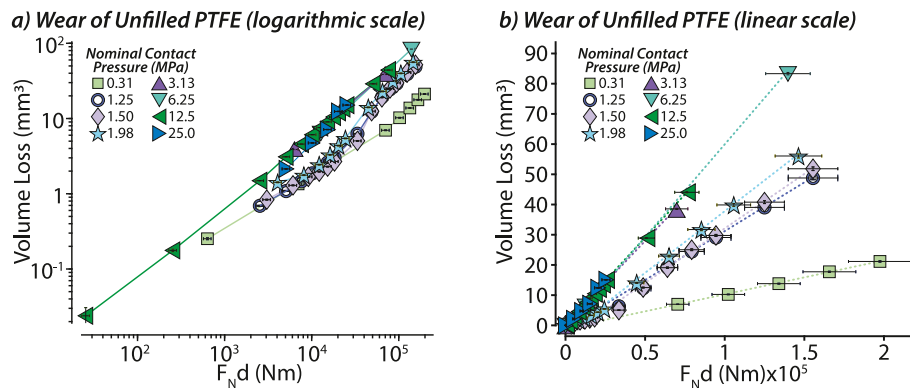


Fig. 3. Wear of unfilled PTFE using a broad range of nominal contact pressures (Actual contact pressure discussed in results). a) Volume loss is plotted as a function of $F_N d$ on a logarithmic scale; connecting lines in (a) are for visualization purposes. b) Volume loss is plotted as a function of $F_N d$; Dotted lines in (b) represent fits for steady-state wear rates.

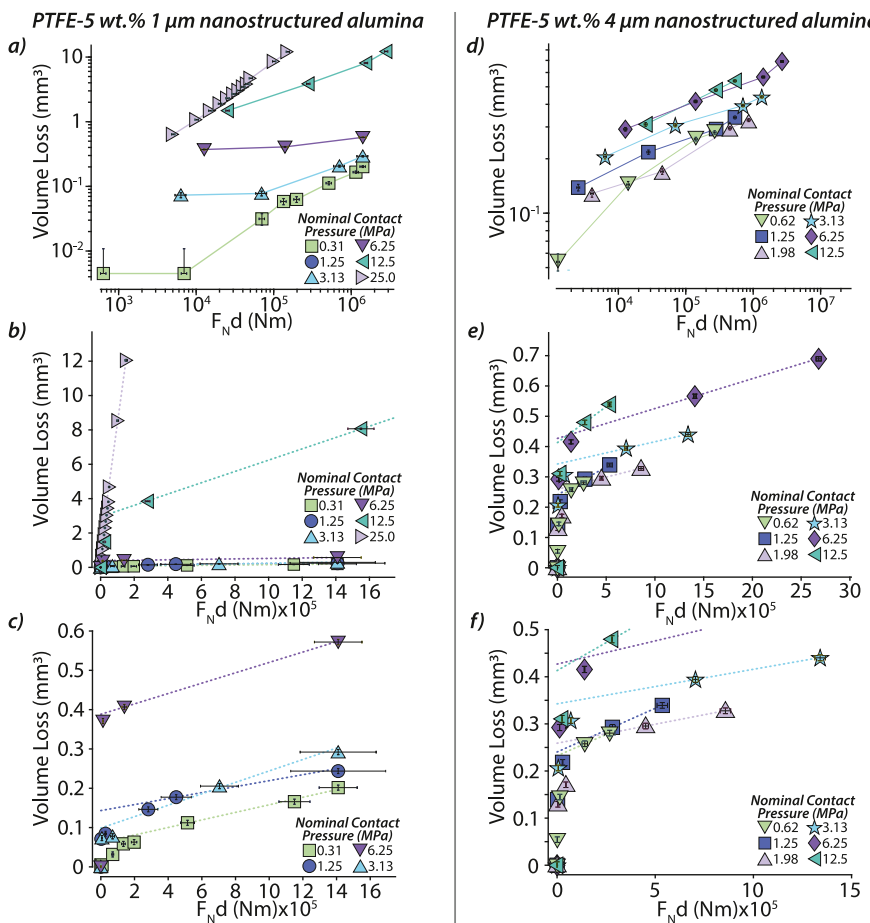


Fig. 4. Wear of PTFE filled with 5 wt% nanostructured 1 μm alumina (a-c) and nanostructured 4 μm alumina (d-f) using a broad range of nominal contact pressures (Actual contact pressure discussed in results). a,d) Volume loss is plotted as a function of $F_N d$ on a logarithmic scale; connecting lines in (a) are for visualization purposes. b,e) Volume loss is plotted as a function of $F_N d$ on a linear scale. c,f) a closer look at wear behavior in low volume loss region. Dotted lines in (b, c, e & f) represent fits for steady-state wear rates.

the correction of contact pressure values to reflect the real measured loading and contact area of the sample. All contact pressure values plotted are adjusted as such, reflecting a contact area closer to the apparent contact of the plastically deformed sample, as samples tested above 6.25 MPa of contact pressure experienced sample creep and an increase in apparent contact area.

An example of the dimensional changes caused by these pressures can be observed by comparing the images of the wear surface of the PTFE-5 wt% nanostructured 1 μm alumina nanocomposite after sliding at 1.25 MPa (Fig. 5a) to those at 12.5 MPa (Fig. 5b). Both samples were initially machined to approximately the same cross-sectional

dimensions of $\sim 6.4 \times 6.4 \text{ mm}^2$. The sample loaded at 1.25 MPa experienced little to no observable dimensional changes while the sample loaded at 12.5 MPa expanded to $8.16 \times 7.44 \text{ mm}^2$ (a 50% increase in nominal contact area); this is even more evident when viewing the polymer sample tested at 12.5 MPa from the side (Fig. 5c). The contact areas of the PTFE-5wt% nanostructured 4 μm alumina samples were also measured after testing, and experienced increases in contact area of 47% at 12.5 MPa ($\sim 6.35 \times 6.40 \text{ mm}^2$ to $8.27 \times 7.10 \text{ mm}^2$) and 136% at 25 MPa ($\sim 6.34 \times 6.38 \text{ mm}^2$ to $10.19 \times 9.38 \text{ mm}^2$). The majority of the sample creep occurred in the first few hundred sliding cycles, and these significant increases in contact area led to the decrease of the actual

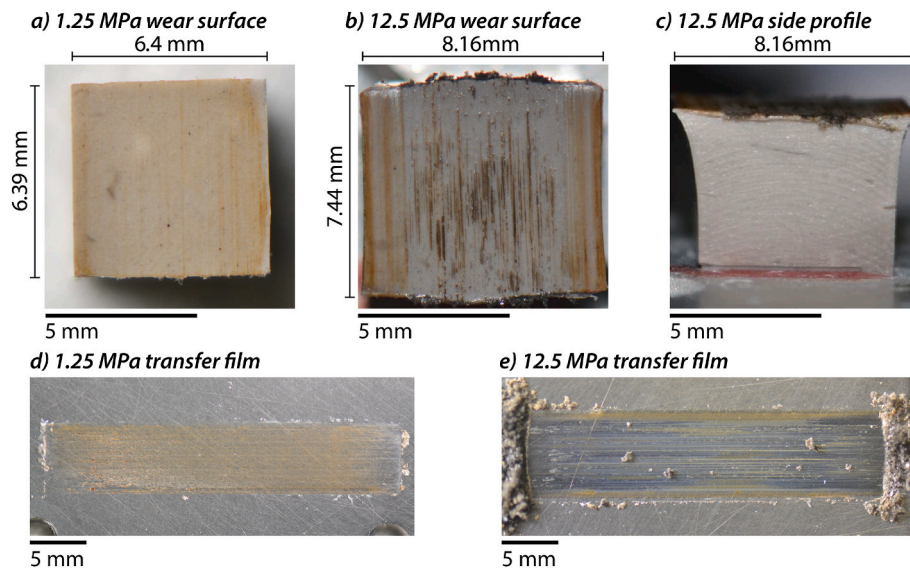


Fig. 5. Images of worn polymer surface and transfer films generated during sliding of PTFE and 5 wt percent alumina composites on steel for various nominal contact pressures.

contact pressure the samples experienced. A nominal contact pressure of 12.5 MPa resulted in a real contact pressure of ~ 8.5 MPa, and a nominal contact pressure of 25 MPa resulted in a real contact pressure of ~ 10.5 MPa. This limitation in contact pressure is due to the yield stress of PTFE, and testing these materials at contact pressures exceeding the yield stress will lead to severe sample creep [49].

The average friction coefficient of each sliding cycle was recorded and plotted over the total sliding distance for PTFE filled with nanostructured 4 μ m alumina to observe changes in friction over distance/testing duration (Fig. 6a). There is a clear trend that with decreasing contact pressure, the friction coefficient increases for samples tested in the 0.62–12.5 MPa nominal contact pressure range. All samples underwent a run-in period in the first 1 km of sliding, after which friction coefficients appear to level out and slowly increase over the duration of testing. Jumps in the friction data indicate an intermittent massing point during testing, where sliding was stopped to perform a mass measurement, after which testing resumes and the samples undergo a much shorter run-in period and return to their previous friction coefficient.

To visualize the relationship between contact pressure and friction coefficient, the average steady state friction coefficient from the last 2 km of sliding was plotted against the contact pressure (Fig. 6b). It should be noted that the nominal contact pressure is described in the legend, while the actual, measured contact pressure is plotted. The average

steady-state friction coefficient of unfilled PTFE was also plotted for comparison. For the unfilled PTFE samples, the friction coefficient appears to be largely unaffected by the change in contact pressure, with all contact pressures exhibiting coefficients of friction near ~ 0.13 . For the PTFE-alumina composite however, the lower contact pressure samples have the highest friction coefficients, and the friction coefficients taper off non-linearly when approaching higher contact pressures. This change in friction coefficient as a result of contact pressure is likely due to the presence of tribofilms at the sliding interface. PTFE-alumina tribofilms have been found to have higher surface energy than PTFE [50]. This higher surface energy is thought to contribute to the increase in friction coefficient observed when tribofilms are formed on the sliding surfaces [26,51]. Two likely sources of this higher surface energy are 1) tribochemically-generated carboxylate end groups in the tribofilms, which bond to the surface they are sliding against and 2) accumulation of metals and metal oxides (transfer from the counter sample and accumulation of alumina fillers).

In order to determine the effects of variations in contact pressure during testing on the friction coefficients of PTFE alumina composites, after testing was concluded on the samples shown in Fig. 6a (~ 10 km of sliding), the same samples were tested for an additional 1.2 km of sliding with incremental changes in the contact pressure (Fig. 7). Samples were allowed to run in for ~ 0.35 km of sliding until friction coefficients

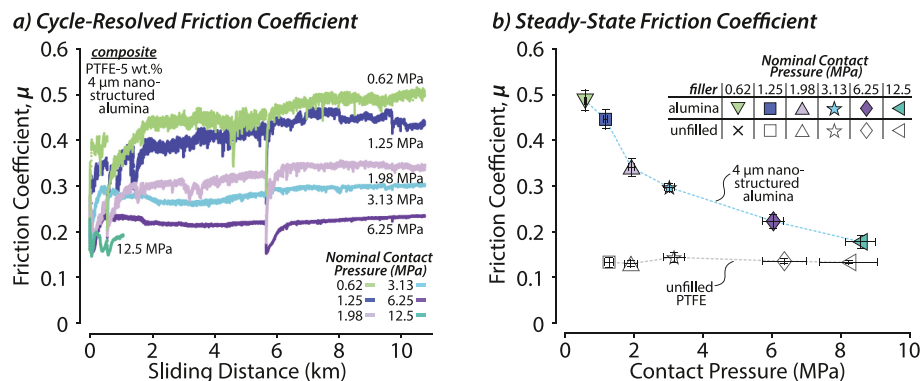


Fig. 6. a) Measured friction coefficient for PTFE filled with 5 wt% nanostructured 4 μ m alumina at nominal contact pressures of 0.62, 1.25, 1.98, 3.13, 6.25, and 12.5 MPa (Actual contact pressure discussed in results). b) Steady state friction coefficient measured at each nominal contact pressure for PTFE filled with 5 wt% nanostructured 4 μ m alumina and unfilled PTFE. Contact pressure plotted is calculated using the measured contact area of the sample and measured normal load.

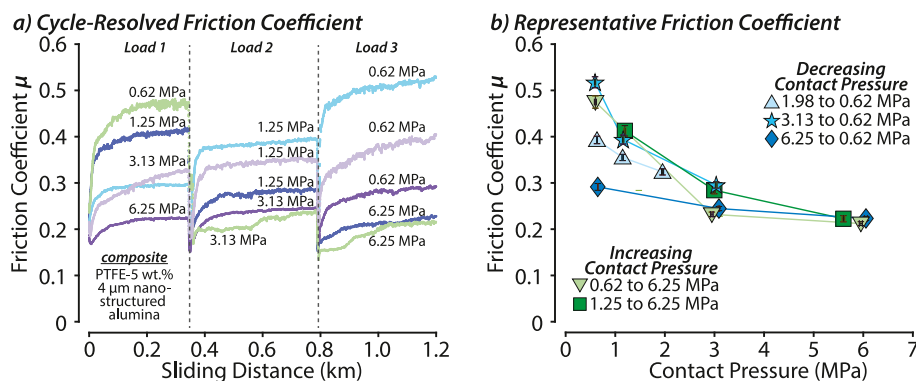


Fig. 7. a) Measured friction coefficient for PTFE filled with 5 wt% nanostructured 4 μ m alumina tested using starting nominal contact pressures of 0.62, 1.25, 1.98, 3.13, and 6.25 MPa. Samples were run-in until friction reached a steady state, then load was increased or decreased (depending on the sample) to change contact pressure. b) Representative friction coefficient selected for each loading region plotted against contact pressure. Contact pressure plotted is calculated using the measured contact area of the sample and measured normal load.

achieved a steady value. For samples with initial contact pressures of 0.62 and 1.25 MPa, the pressure was increased to 3.13 MPa for an additional ~ 0.4 km of sliding (Fig. 7a, Load 2) without stopping the test. For samples with initial contact pressures of 1.98, 3.13, and 6.25 MPa, the pressure was decreased to 1.25 MPa for ~ 0.4 km of sliding (Fig. 7a, Load 2) without stopping the test. After this second loading region, the sample contact pressures were adjusted again, increasing the 3.13 MPa samples to 6.25 MPa and decreasing the 1.25 MPa samples to 0.62 MPa and were tested for an additional 0.4 km of sliding (Fig. 7a, Load 3).

For all samples tested with an increasing contact pressure over the course of the load variation test, the friction coefficients of the samples decreased. The opposite was true for samples with decreasing loads, where the lower contact pressure corresponded to increases in friction coefficient. The overall trend of this testing data set is shown in Fig. 7b, which closely matches friction coefficient and contact pressure trend established in Fig. 6b. However, the amount by which the friction coefficient increased or decreased for each sample was not the same and was not proportional to the original contact pressure at which it was tested. For the sample that was decreased from 3.13 MPa to 0.62 MPa, the final friction coefficient of the sample was higher than the sample initially tested at 0.62 MPa, a 70% increase from its original friction coefficient. However, for the sample that was decreased from 6.25 MPa to 0.62 MPa, the final friction coefficient was only 30% higher than its original friction coefficient.

While all samples tested in the high contact pressure range (6.25 MPa) have converging friction coefficients, it appears at lower loadings, there are larger variations. The behavior of these samples in response to load variation appears to be very dependent on the history of the sample, such as its starting friction coefficient and its tribofilm development. For samples with more robust tribofilms, their load variation response could be quite different than a sample with less robust films. In addition, it also indicates that load variation during a component's lifetime could have significant ($>50\%$) variations in the friction coefficient of the system simply by changing the system contact pressure.

IR spectra of the polymer wear surfaces of PTFE filled with 5 wt% 4 μ m nanostructured alumina were collected after testing at nominal contact pressures of 0.62, 3.13, 6.25, and 12.5 MPa. Absorbance spectra were normalized to the 1149 cm^{-1} peak, which is CF_2 , a characteristic peak of PTFE (Fig. 8). All samples showed accumulation of metal oxides in the 800 cm^{-1} region, with a trend of higher levels of metal oxides at higher pressures [46]. Carboxylates were found in the polymer wear surfaces of all samples, as indicated by the carboxylate peaks at 1660 cm^{-1} and 1430 cm^{-1} [26–29, 52–54]. However, it appears that the level of carboxylates in the low contact pressure sample (0.62 MPa) is the lowest of all samples measured. It is possible that in order to increase the level of carboxylates present, the 0.62 MPa sample would have to slide a further distance than samples tested at higher pressures in order to accumulate equivalent carboxylates. Alternatively, the 0.62 MPa sample had the highest friction coefficient of all samples tested (~ 0.5), and appeared to cause minor scratches in counter sample during sliding,

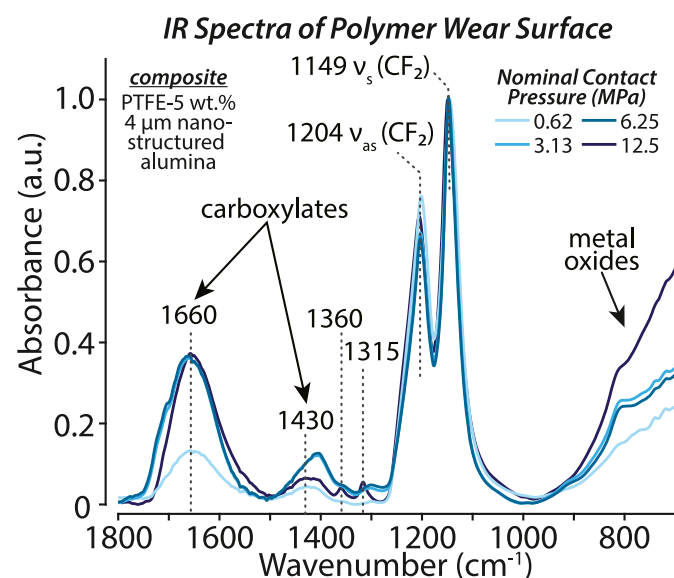


Fig. 8. IR spectra of the polymer wear surfaces of PTFE filled with 5 wt% 4 μ m nanostructured alumina tested at nominal contact pressures of 0.62, 3.13, 6.25, and 12.5 MPa. Absorbance was normalized to the 1149 cm^{-1} CF_2 peak.

which may have resulted in instability of the tribofilms, leading to some film delamination. The ultralow wear achieved by this sample ($K \sim 1.8 \times 10^{-7}\text{ mm}^3/\text{Nm}$), comparable to the wear of the highest load sample ($K \sim 2.4 \times 10^{-7}\text{ mm}^3/\text{Nm}$), indicates that sufficient tribofilm formation has occurred to promote low wear.

For samples tested at 3.13, 6.25, and 12.5 MPa, the level of carboxylates at the 1660 cm^{-1} peak were very similar. The 12.5 MPa sample was only slid for $\sim 10\%$ of the sliding distance of the other samples, and the comparable level of carboxylates measured may be due to the very high contact pressure the sample experienced resulting in a high F_{ND} . The 12.5 MPa sample also had distinct peaks at 1360 and 1315 cm^{-1} , which are found when significantly shortened PTFE chains are present [48, 55, 56]. The high loading of this sample may have contributed to the increased level of shortened chains present in the polymer wear surface. However, the 12.5 MPa sample had a smaller peak at 1430 cm^{-1} when compared to the 3.13 and 6.25 MPa samples, indicating a lower level of chelated carboxylic acids [26–29, 52–54]. Tribofilms form and carboxylates accumulate at all contact pressures tested, and this formation at a large range of loading contributes to the low wear rates achieved by all PTFE-5 wt% 4 μ m nanostructured alumina samples tested.

4.4. Wear of PTFE filled with 0.5 μm alumina

As previously stated, PTFE filled with 0.5 μm alumina was selected because of reports that it only produces marginal reductions in the wear rate of PTFE and does not compete with the three to four order of magnitude reduction observed with nanostructured 1 μm and 4 μm alumina composites. Volume loss due to wear is shown as a function of F_{Nd} (Fig. 9) for PTFE filled with 5 wt% 0.5 μm alumina when subjected to various contact pressures. As shown in Fig. 9a and b, the sample tested at 6.25 MPa had a much higher amount of volume loss ($\sim 100x$) compared to the lower contact pressure samples over the same F_{Nd} . In contrast, the samples tested at 0.31 MPa and 1.25 MPa overlap in the ~ 0.5 to 2 Nm range (Fig. 9c), with nearly identical trends in volume loss. This indicates that at pressures within this low range, the 0.5 μm alumina samples are unaffected by contact pressure variation.

This wear behavior does differ from the idealized case shown in Fig. 1c, as there is not a constant linear wear rate and both samples exhibit run in during early sliding cycles. However, it does appear that in the lower contact pressures of 0.31 and 1.25 MPa, the volume loss vs. F_{Nd} data overlaps on one curve. This suggests that the run-in transition is a linear function of both cycles and the applied normal load. As such, it seems that this composite just depends on accumulation of tribofilms. As these alumina particles are smaller and fully dense, we theorize that they accumulate in the tribofilms without the need to fracture into smaller particles as reported for the other types of nanostructured alumina [32]. While this results in low wear rates, they are still never as low as the wear rates observed by the friable nanostructured 4 μm alumina-filled PTFE composites. We hypothesize that the inability to break down into smaller fragments will prevent these fillers from achieving lower wear rates, as the alumina that accumulates at the sliding interface will be the primary particle size and can lead to high stress abrasive interactions with tribofilms on the counter surface material.

While the 0.5 μm dense alumina fillers do not need to be friable to achieve low wear rates at lower pressures, their smaller size makes them less effective as a mechanical reinforcing filler (as discussed when comparing the 1 and 4 μm alumina-filled composites). The 0.5 μm alumina PTFE composite slid at 6.25 MPa exhibits a high, linear wear rate almost immediately, exhibiting no run-in transition. From this, we see that the overall load carrying ability increases with the actual size of the particle, as the PTFE filled with 5 wt % 0.5 μm alumina transitions to a higher wear at a lower pressure than the 1 μm alumina, which transitions to a higher wear rate at a lower pressure than the 4 μm alumina. Overall, there must be a balance in the particles' primary size as well as its ability to fracture and accumulate at the interface. It seems that smaller particles might facilitate less run-in volume, while larger particles will help facilitate mechanical reinforcement. A unique combination was found in the nanostructured 4 μm alumina particles, in that they are large enough in the bulk to reinforce mechanically yet can break up into small particles and accumulate in protective tribofilms.

5. Conclusions

The wear behavior of PTFE-alumina composites was found to vary based on filler type (dense vs nanostructured) and applied contact pressure during testing. PTFE filled with 0.5 μm alumina achieved low wear rates only at the lower range of contact pressures tested, with a transition to high wear at contact pressures > 1.25 MPa. PTFE filled with nanostructured alumina fillers demonstrated contact pressure dependence in both wear rate and friction coefficient. PTFE filled with 1 μm nanostructured alumina achieved low wear at contact pressures between 0.31 and 6.25 MPa, but transition to high wear at higher contact pressures. When tested at contact pressures ranging from 0.62 to 8.5 MPa, PTFE filled with 4 μm nanostructured alumina achieved ultralow wear rates from 7×10^{-8} to 2×10^{-7} mm^3/Nm . The steady-state wear rate of the PTFE filled with 4 μm nanostructured alumina remained low, even when sliding was performed at contact pressures at or exceeding

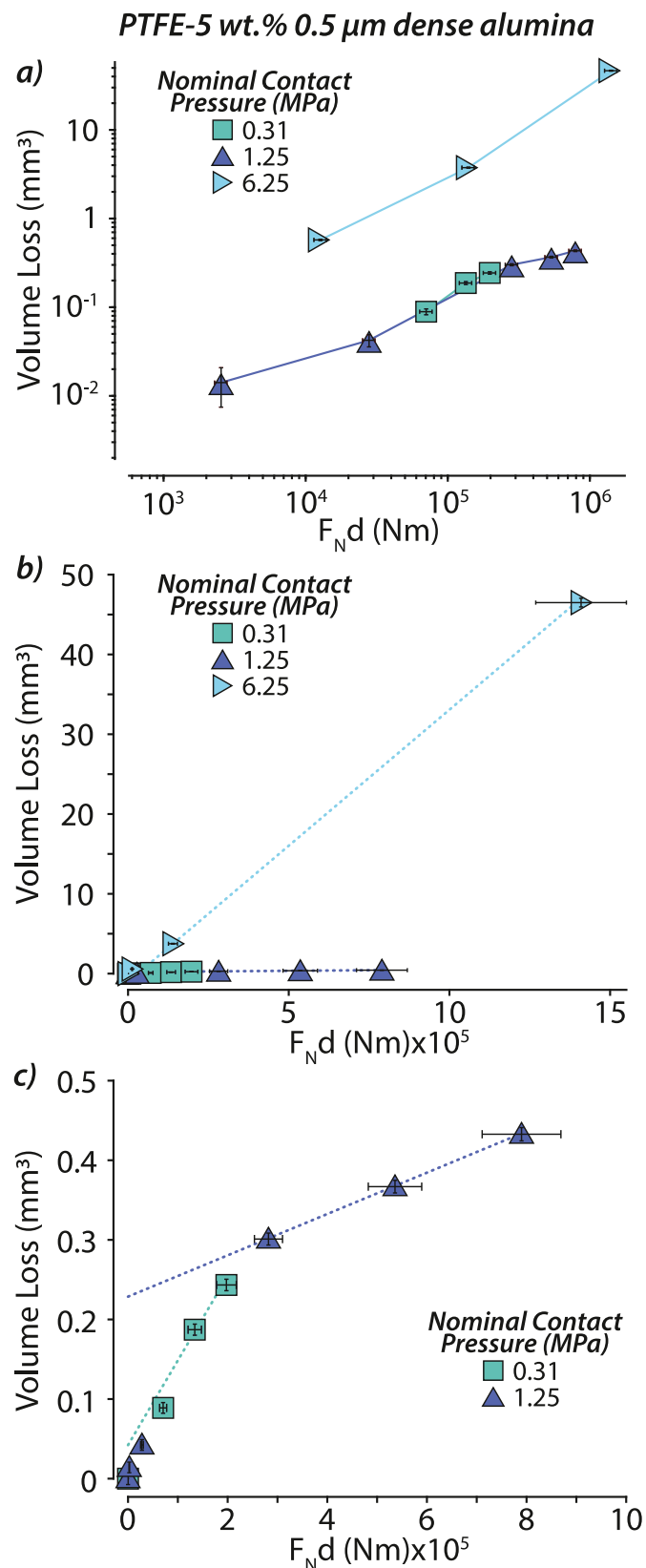


Fig. 9. Wear of PTFE filled with 5 wt% 0.5 μm alumina using nominal contact pressures of 0.31, 1.25 and 6.25 MPa. a) Volume loss is plotted as a function of F_{Nd} on a logarithmic scale; connecting lines in (a) are for visualization purposes. b) Volume loss is plotted as a function of F_{Nd} on a linear scale. c) A closer look at wear behavior in low volume loss region. Dotted lines in (b and c) represent fits for steady-state wear rates.

the flow stress of the polymer. IR spectroscopy indicated that tribofilms rich in carboxylates and metal oxides form at the sliding interface, even at low contact pressures, and promote ultralow wear behavior in the full range of contact pressures tested. The friction coefficients of the PTFE-5 wt% 4 μ m alumina samples were observed to decrease with increasing contact pressure, reaching friction coefficients as high as 0.5 and as low as 0.17. This dramatic difference in friction coefficient was investigated through contact pressure variation experiments, which demonstrated that if the contact pressure is incrementally changed during testing, the sample can experience up to a 70% increase or decrease in friction coefficient. The observed change in friction coefficient due to contact pressure variation does not appear to scale directly with pressure, and instead is heavily dependent on the history of the sample, such as its initial friction coefficient and its tribofilm development.

Declaration of competing interest

The authors declare that they have no known competing financial interests or personal relationships that could have appeared to influence the work reported in this paper.

Acknowledgements

The authors would like to thank the many collaborators for their thoughtful comments and insight, including Christopher P. Junk, Gregory S. Blackman and Heidi Burch at DuPont. We also thank Shefik Bowen and Daniel Hallinan at FAMU-FSU for access and training to ATR-IR spectroscopy. All the authors acknowledge. This material is based upon work supported by the National Science Foundation (NSF), including the Civil, Mechanical and Manufacturing Innovation (CMMI) under Grant #2027029 and #1463141 (Krick), as well as NSF Graduate Research Fellowship Program under Grant #1449440 (Van Meter).

References

- [1] M.M. Renfrew, E.E. Lewis, Polytetrafluoroethylene. Heat resistant, chemically inert plastic, Ind. Eng. Chem. 38 (9) (Sep. 1946) 870–877, <https://doi.org/10.1021/IE50441A009>.
- [2] K. V Shooter, D. Tabor, The frictional properties of plastics, Proc. Phys. Soc. B 65 (9) (Sep. 1952) 661, <https://doi.org/10.1088/0370-1301/65/9/302>.
- [3] R.F. King, D. Tabor, The effect of temperature on the mechanical properties and the friction of plastics, Proc. Phys. Soc. B 66 (9) (Sep. 1953) 728, <https://doi.org/10.1088/0370-1301/66/9/302>.
- [4] D.G. Flom, N.T. Porile, Friction of Teflon sliding on Teflon, J. Appl. Phys. 26 (9) (May 2004) 1088, <https://doi.org/10.1063/1.1722156>.
- [5] G. Deli, X. Qunji, W. Hongli, Study of the wear of filled polytetrafluoroethylene, Wear 134 (2) (Nov. 1989) 283–295, [https://doi.org/10.1016/0043-1648\(89\)90131-2](https://doi.org/10.1016/0043-1648(89)90131-2).
- [6] T.A. Blanchet, F.E. Kennedy, Sliding wear mechanism of polytetrafluoroethylene (PTFE) and PTFE composites, Wear 153 (1) (Mar. 1992) 229–243, [https://doi.org/10.1016/0043-1648\(92\)90271-9](https://doi.org/10.1016/0043-1648(92)90271-9).
- [7] W.G. Sawyer, K.D. Freudenberg, P. Bhimaraj, L.S. Schadler, A study on the friction and wear behavior of PTFE filled with alumina nanoparticles, Wear 254 (5–6) (Mar. 2003) 573–580, [https://doi.org/10.1016/S0043-1648\(03\)00252-7](https://doi.org/10.1016/S0043-1648(03)00252-7).
- [8] K. Tanaka, S. Kawakami, Effect of various fillers on the friction and wear of polytetrafluoroethylene-based composites, Wear 79 (2) (Jul. 1982) 221–234, [https://doi.org/10.1016/0043-1648\(82\)90170-3](https://doi.org/10.1016/0043-1648(82)90170-3).
- [9] S. Bahadur, D. Tabor, The wear of filled polytetrafluoroethylene, Wear 98 (C) (Nov. 1984) 1–13, [https://doi.org/10.1016/0043-1648\(84\)90213-8](https://doi.org/10.1016/0043-1648(84)90213-8).
- [10] G. De-Li, Z. Bing, X. Qun-Ji, W. Hong-Li, Effect of tribocochemical reaction of polytetrafluoroethylene transferred film with substrates on its wear behaviour, Wear 137 (2) (May 1990) 267–273, [https://doi.org/10.1016/0043-1648\(90\)90139-2](https://doi.org/10.1016/0043-1648(90)90139-2).
- [11] Z.-Z. Zhang, Q.-J. Xue, W.-M. Liu, W.-C. Shen, Friction and wear characteristics of metal sulfides and graphite-filled PTFE composites under dry and oil-lubricated conditions, J. Appl. Polym. Sci. 72 (May 1999) [Online]. Available: [https://onlinelibrary.wiley.com/doi/10.1002/\(SICI\)1097-4628\(19990509\)72:6/3C751::AID-APP3%3E3.0.CO;2-W](https://onlinelibrary.wiley.com/doi/10.1002/(SICI)1097-4628(19990509)72:6/3C751::AID-APP3%3E3.0.CO;2-W).
- [12] F. Li, F.Y. Yan, L.G. Yu, W.M. Liu, The tribological behaviors of copper-coated graphite filled PTFE composites, Wear 237 (1) (Jan. 2000) 33–38, [https://doi.org/10.1016/S0043-1648\(99\)00303-8](https://doi.org/10.1016/S0043-1648(99)00303-8).
- [13] F. Li, K. ao Hu, J. lin Li, B. yuan Zhao, The friction and wear characteristics of nanometer ZnO filled polytetrafluoroethylene, Wear 249 (10–11) (Nov. 2001) 877–882, [https://doi.org/10.1016/S0043-1648\(01\)00816-X](https://doi.org/10.1016/S0043-1648(01)00816-X).
- [14] J. Khedkar, I. Negulescu, E.I. Meletis, Sliding wear behavior of PTFE composites, Wear 252 (5–6) (Mar. 2002) 361–369, [https://doi.org/10.1016/S0043-1648\(01\)00859-6](https://doi.org/10.1016/S0043-1648(01)00859-6).
- [15] W.X. Chen, et al., Tribological behavior of carbon-nanotube-filled PTFE composites, Tribol. Lett. 15 (3) (Oct. 2003) 275–278, <https://doi.org/10.1023/A:1024869305259>, 2003 153.
- [16] N.V. Klaas, K. Marcus, C. Kellock, The tribological behaviour of glass filled polytetrafluoroethylene, Tribol. Int. 38 (9) (Sep. 2005) 824–833, <https://doi.org/10.1016/J.TRIPOINT.2005.02.010>.
- [17] D.L. Burris, W.G. Sawyer, Improved wear resistance in alumina-PTFE nanocomposites with irregular shaped nanoparticles, Wear 260 (2006) 915–918, <https://doi.org/10.1016/j.wear.2005.06.009>.
- [18] S.Q. Lai, L. Yue, T.S. Li, Z.M. Hu, The friction and wear properties of polytetrafluoroethylene filled with ultrafine diamond, Wear 260 (4–5) (Feb. 2006) 462–468, <https://doi.org/10.1016/J.WEAR.2005.03.010>.
- [19] S.E. McElwain, T.A. Blanchet, L.S. Schadler, W.G. Sawyer, Effect of Particle Size on the Wear Resistance of Alumina-Filled PTFE Micro- and Nanocomposites, May 2008, pp. 247–253, <https://doi.org/10.1080/10402000701730494>, 10.1080/10402000701730494, vol. 51, no. 3.
- [20] D.L. Burris, et al., A route to wear resistant PTFE via trace loadings of functionalized nanofillers, Wear 267 (2009) 653–660, <https://doi.org/10.1016/j.wear.2008.12.116>.
- [21] T.A. Blanchet, S.S. Kandanur, L.S. Schadler, Coupled effect of filler content and countersurface roughness on PTFE nanocomposite wear resistance, Tribol. Lett. 40 (1) (Oct. 2010) 11–21, <https://doi.org/10.1007/S11249-009-9519-2/FIGURES/16>.
- [22] D.L. Burris, B. Boesl, G.R. Bourne, W.G. Sawyer, Polymeric nanocomposites for tribological applications, Macromol. Mater. Eng. 292 (4) (Apr. 2007) 387–402, <https://doi.org/10.1002/mame.200600416>.
- [23] D.L. Burris, W.G. Sawyer, Tribological sensitivity of PTFE/alumina nanocomposites to a range of traditional surface finishes, Tribol. Trans. 48 (2) (Apr. 2005) 147–153, <https://doi.org/10.1080/05698190590923842>.
- [24] B.A. Krick, J.J. Ewin, G.S. Blackman, C.P. Junk, W. Gregory Sawyer, W.G. Sawyer, Environmental dependence of ultra-low wear behavior of polytetrafluoroethylene (PTFE) and alumina composites suggests tribochemical mechanisms, Tribology Int 51 (Jul. 2012) 42–46, <https://doi.org/10.1016/j.triboint.2012.02.015>.
- [25] K.I. Alam, A. Baratz, D. Burris, Leveraging trace nanofillers to engineer ultra-low wear polymer surfaces, Wear 482 (483) (Oct. 2021), 203965, <https://doi.org/10.1016/J.WEAR.2021.203965>.
- [26] K.E. Van Meter, C.P. Junk, K.L. Campbell, T.F. Babuska, B.A. Krick, Ultralow wear self-mated PTFE composites, Macromolecules (May 2022), <https://doi.org/10.1021/ACS.MACROMOL.1C02581>.
- [27] K.L. Campbell, et al., Ultralow wear PTFE-based polymer composites -the role of water and tribochemistry, Macromolecules 52 (14) (2019) 5268–5277, Jul, <https://doi.org/10.1021/acs.macromol.9b00316>.
- [28] A.A. Pitenis, et al., Ultralow wear PTFE and alumina composites: it is all about tribochemistry, Tribol. Lett. 57 (1) (2015), <https://doi.org/10.1007/s11249-014-0445-6>.
- [29] K.L. Harris, et al., PTFE tribology and the role of mechanochemistry in the development of protective surface films, ACS Macromol 48 (2015), <https://doi.org/10.1021/acs.macromol.5b00452>.
- [30] B.A. Krick, J.J. Ewin, E.J. McCumiskey, Tribofilm Formation and run-in behavior in ultra-low-wearing polytetrafluoroethylene (PTFE) and alumina nanocomposites, Tribol. Trans. 57 (6) (2014) 1058–1065, Nov, <https://doi.org/10.1080/10402004.2014.933934>.
- [31] M.A. Sidebottom, T.F. Babuska, S. Ullah, N. Heckman, B.L. Boyce, B.A. Krick, Nanomechanical filler functionality enables ultralow wear polytetrafluoroethylene composites, ACS Appl. Mater. Interfaces (2022), <https://doi.org/10.1021/acsami.2c13644>.
- [32] B.A. Krick, et al., Ultralow wear fluoropolymer composites: nanoscale functionality from microscale fillers, Tribol. Int. 95 (Mar. 2016) 245–255, <https://doi.org/10.1016/J.TRIPOINT.2015.10.002>.
- [33] Y. Uchiyama, K. Tanaka, Wear laws for polytetrafluoroethylene, Wear 58 (2) (Feb. 1980) 223–235, [https://doi.org/10.1016/0043-1648\(80\)90152-0](https://doi.org/10.1016/0043-1648(80)90152-0).
- [34] J. Ye, H.S. Khare, D.L. Burris, Quantitative characterization of solid lubricant transfer film quality, Wear 316 (1–2) (Aug. 2014) 133–143, <https://doi.org/10.1016/J.WEAR.2014.04.017>.
- [35] A.A. Pitenis, J.J. Ewin, K.L. Harris, W.G. Sawyer, B.A. Krick, In vacuo tribological behavior of polytetrafluoroethylene (PTFE) and alumina nanocomposites: the importance of water for ultralow wear, Tribol. Lett. 53 (1) (2014) 189–197 [Online]. Available: <https://link.springer.com/article/10.1007/s11249-013-0256-1>.
- [36] J. Ye, H.S. Khare, D.L. Burris, Transfer film evolution and its role in promoting ultra-low wear of a PTFE nanocomposite, Wear 297 (2013), <https://doi.org/10.1016/j.wear.2012.12.002>, 1–2.
- [37] D.L. Burris, W.G. Sawyer, A low friction and ultra low wear rate PEEK/PTFE composite, Wear 261 (3–4) (Aug. 2006) 410–418, <https://doi.org/10.1016/j.wear.2005.12.016>.
- [38] J.R. Vail, B.A. Krick, K.R. Marchman, W.G. Sawyer, Polytetrafluoroethylene (PTFE) fiber reinforced polyetheretherketone (PEEK) composites, Wear 270 (11–12) (May 2011) 737–741.
- [39] T.L. Schmitz, J.E. Action, D.L. Burris, J.C. Ziegert, W.G. Sawyer, Wear-rate uncertainty analysis, J. Tribol. 126 (4) (Oct. 2004) 802–808, <https://doi.org/10.1115/1.1792675>.

[40] T.L. Schmitz, J.E. Action, J.C. Ziegert, W.G. Sawyer, The difficulty of measuring low friction: uncertainty analysis for friction coefficient measurements, *J. Tribol.* 127 (3) (Jul. 2005) 673–678, <https://doi.org/10.1115/1.1843853>.

[41] D.L. Burris, W.G. Sawyer, Tribological behavior of PEEK/PTFE surfaces, *Wear* 262 (1–2) (Jan. 2007) 220–224, <https://doi.org/10.1016/J.WEAR.2006.03.045>.

[42] D.L. Burris, W.G. Sawyer, Measurement uncertainties in wear rates, *Tribol. Lett.* 36 (1) (Oct. 2009) 81–87, <https://doi.org/10.1007/S11249-009-9477-8/FIGURES/2>.

[43] D.L. Burris, Investigation of the Tribological Behavior of Polytetrafluoroethylene at Cryogenic Temperatures, Jan. 2008, pp. 92–100, <https://doi.org/10.1080/10402000701660618>, vol. 51, no. 1.

[44] J.F. Archard, Contact and rubbing of flat surfaces, *J. Appl. Phys.* 24 (8) (Aug. 1953) 981–988, <https://doi.org/10.1063/1.1721448>.

[45] J. Ye, A.C. Moore, D.L. Burris, Transfer film tenacity: a case study using ultra-low-wear alumina-PTFE, *Tribol. Lett.* 59 (3) (Sep. 2015) 1–11, <https://doi.org/10.1007/S11249-015-0576-4/FIGURES/8>.

[46] M.A. Sidebottom, et al., Perfluoroalkoxy (PFA)- α -Alumina composites: effect of environment on tribological performance, *Tribol. Lett.* 68 (1) (Mar. 2020) 14, <https://doi.org/10.1007/S11249-019-1257-5>.

[47] K.I. Alam, A. Dorazio, D.L. Burris, Polymers tribology exposed: eliminating transfer film effects to clarify ultralow wear of PTFE, *Tribol. Lett.* 68 (2) (Jun. 2020) 1–13, <https://doi.org/10.1007/S11249-020-01306-9/TABLES/2>.

[48] H.S. Khare, et al., Interrelated effects of temperature and environment on wear and tribochemistry of an ultralow wear PTFE composite, *J. Phys. Chem. C* 119 (29) (Jul. 2015) 16518–16527, <https://doi.org/10.1021/ACS.JPCC.5B00947>.

[49] P.J. Rae, D.M. Dattelbaum, The properties of poly(tetrafluoroethylene) (PTFE) in compression, *Polymer* 45 (22) (2004) 7615–7625, Oct, <https://doi.org/10.1016/J.POLYMER.2004.08.064>.

[50] J. Ye, et al., Interfacial gradient and its role in ultralow wear sliding, *J. Phys. Chem.* (2020), <https://doi.org/10.1021/acs.jpcc.9b12036>.

[51] D.L. Burris, *Effects of Nanoparticles on the Wear Resistance of Polytetrafluoroethylene*, University of Florida, Gainesville, 2007.

[52] M. Przedlacki, C. Kajdas, Tribochemistry of fluorinated fluids hydroxyl groups on steel and aluminum surfaces, *Tribol. Trans.* 49 (2) (2006) 202–214, <https://doi.org/10.1080/05698190500544676>.

[53] C.K. Kajdas, Importance of the triboemission process for tribochemical reaction, *Tribol. Int.* 38 (3) (Mar. 2005) 337–353, <https://doi.org/10.1016/J.TRIPOINT.2004.08.017>.

[54] D.R. Haidar, K.I. Alam, D.L. Burris, Tribological insensitivity of an ultralow-wear poly(etheretherketone)-polytetrafluoroethylene polymer blend to changes in environmental moisture, *J. Phys. Chem. C* 122 (10) (2018) 5518–5524, Mar, <https://doi.org/10.1021/acs.jpcc.7b12487>.

[55] H. Vanni, J.F. Rabolt, Fourier transform infrared investigation of the effects of irradiation on the 19 and 30°C phase transitions in polytetrafluoroethylene, *J. Polym. Sci. Polym. Phys. Ed* 18 (3) (Mar. 1980) 587–596, <https://doi.org/10.1002/POL.1980.180180317>.

[56] J.L. Lauer, B.G. Bunting, W. R J Jr., Investigation of frictional transfer films of PTFE by infrared emission spectroscopy and phase-locked ellipsometry, *Tribol. Trans.* 31 (2) (1988) 282–288, <https://doi.org/10.1080/10402008808981824>.